THE JOURNAL OF BIOLOGICAL CHEMISTRY VOL. 283, NO. 43, pp. 28860–28872, October 24, 2008

A Novel Splicing Variant of Mouse Interleukin (IL)-24 Antagonizes IL-24-induced Apoptosis*[S]

Received for publication, April 1, 2008, and in revised form, July 17, 2008 Published, JBC Papers in Press, August 15, 2008, DOI 10.1074/jbc.M802510200

Anupama Sahoo[‡], Yun Min Jung[‡], Ho-Keun Kwon[‡], Hwa-Jung Yi[‡], Suho Lee[‡], Sunghoe Chang[‡], Zee-Yong Park[‡], Ki-Chul Hwang[§], and Sin-Hyeog Im[‡¶1]

From the [‡]Department of Life Sciences, Gwangju Institute of Science and Technology, Gwangju 500-712, [§]Cardiovascular Research Institute, Cardiology Division, Yonsei University College of Medicine, Seoul 120-752, and [¶]Center for Distributed Sensor Network, Gwangju Institute of Science and Technology, Gwangju 500-712, Korea

Alternative splicing of mRNA enables functionally diverse protein isoforms to be expressed from a single gene, allowing transcriptome diversification. Interleukin (IL)-24/MDA-7 is a member of the IL-10 gene family, and FISP (IL-4-induced secreted protein), its murine homologue, is selectively expressed and secreted by T helper 2 lymphocytes. A novel splice variant of mouse IL-24/FISP, designated FISP-sp, lacks 29 nucleotides from the 5′-end of exon 4 of FISP. The level of FISP-sp expression is 10% of the level of total primary FISP transcription. Unlike FISP, FISP-sp does not induce growth inhibition and apoptosis. FISP-sp is exclusively localized in endoplasmic reticulum, and its expression is up-regulated by endoplasmic reticulum stress. Our results suggest that the novel splicing variant FISP-sp dimerizes with FISP and blocks its secretion and inhibits FISP-induced apoptosis *in vivo*.

Alternative splicing is a process occurring in eukaryotes, whereby a pre-mRNA transcribed from one gene can be processed into multiple alternative mature mRNA isoforms, thus leading to the formation of a number of different proteins from a single gene (1). The number of transcripts generated is mediated by *cis*-regulatory elements such as the promoter, enhancer, and repressor control. Alternative splicing regulates the structure of transcripts, leading to functional diversification. Transcript variants generated by alternative splicing are often spatially and/or temporally specific, resulting in effects seen only in certain cells or developmental stages (2). Alterations in RNA processing can lead to a variety of human diseases, including cancer (3).

Alternative splicing is tightly regulated to control certain stress conditions. The generation of the alternatively spliced form of HAC-1 (homologue of *Apaf-1* and *ced-4*) or XBP1 (X-box-binding protein 1) is stimulated by the accumulation of unfolded proteins in the endoplasmic reticulum (ER)[2] (3), an event known as "ER stress." The spliced form of XBP1 activates the unfolded protein response (UPR), which actively resolves ER stress (4). In addition, various studies suggest that alternative splicing is precisely and efficiently regulated to fulfill specific tasks (5). Hence, the identification and characterization of splicing variants generated in specific spatial, temporal, or stress conditions are likely to increase our understanding of their functional importance.

Mouse interleukin 24 (mIL-24), also known as FISP (IL-4-induced secreted protein) was identified by representational difference analysis during the isolation of genes selectively expressed in T helper 2 (Th2) cells (6). mIL-24/FISP is a member of the IL-10 family along with IL-10, IL-19, IL-20, and IL-26, and it is selectively expressed in Th2 but not Th1 cells. mIL-24/FISP has significant homology with rat *mob*-5/*c49a* (80% to DNA and 69% to protein) and also with the human melanoma differentiation-associated gene 7 (IL-24/MDA-7; 89% to DNA and 93% to protein(7, 8)). Even though mIL-24/FISP is selectively expressed in Th2 cells, its functional role in Th2 cell development remains unexplored. Many studies have focused on the anti-cancer activity of IL-24/MDA-7 in various types of cancers, including melanoma, breast cancer, lung cancer, ovarian carcinoma, cervical carcinoma, colon carcinoma, prostate carcinoma, hepatoma, pancreatic carcinoma, and osteosarcoma (9–13). Recent studies have demonstrated that the mIL-24/FISP gene suppresses the growth of hepatoma cells *in vivo* after being delivered via intramuscular electroporation (14), suggesting that mIL-24/FISP has anti-tumor activity, and that mIL-24/FISP is truly a homologue of MDA-7.

MDA-7S, a splice variant of MDA-7/IL-24, was identified in normal human melanocytes, and the loss of the splice variant expression was associated with metastatic melanoma (15).

* This work was supported by grants from the 21st Century Frontier Functional Human Genome Project, Korea Health 21 R & D Project, Ministry of Health and Welfare Grant A050533, the KBRDG Initiative Research Program, Grant RTI05-01-01 from the Regional Technology Innovation Program of the MOCIE, and a Systems Biology Infrastructure Establishment grant provided by Gwangju Institute of Science and Technology in 2008. The costs of publication of this article were defrayed in part by the payment of page charges. This article must therefore be hereby marked "*advertisement*" in accordance with 18 U.S.C. Section 1734 solely to indicate this fact.

The nucleotide sequence(s) reported in this paper has been submitted to the GenBank™/EBI Data Bank with accession number(s) AF333251 and DQ401033.

[S] The on-line version of this article (available at http://www.jbc.org) contains supplemental Table 1 and Figs. 1–5.

[1] To whom correspondence should be addressed: Dept. of Life Sciences, Gwangju Institute of Science and Technology, 1 Oryong-dong, Buk-gu, Gwangju 500-712, Korea. Tel.: 82-62-970-2524; Fax: 82-62-970-2484; E-mail: imsh@gist.ac.kr.

[2] The abbreviations used are: ER, endoplasmic reticulum; UPR, unfolded protein response; mIL-24, mouse interleukin 24; FISP, IL-4-induced secreted protein; RT, real time; HEK293, human embryonic kidney 293; DMEM, Dulbecco's modified Eagle's medium; PBS, phosphate-buffered saline; PMA, phorbol 12-myristate 13-acetate; BSA, bovine serum albumin; PDI, protein-disulfide isomerase; ORF, open reading frame; BiP, binding protein; GFP, green fluorescent protein; NMD, nonsense mediated decay; IRE1, inositol-requiring enzyme; ACN, acetonitrile; HA, hemagglutinin.

MDA-7S heterodimerizes with MDA-7 but does not influence the progress of MDA-7/IL-24-induced cell death.

In this study, we identified a novel splicing variant of mouse IL-24/FISP from an activated Th2 cell clone (D10). The splice variant, designated FISP-sp, lacks 29 bp of exon 4 from FISP, resulting in a frameshift. Thus, FISP-sp mRNA encodes a truncated protein of 158 amino acid residues. Unlike FISP, the cytoplasmic localization of the FISP-sp protein appears to be restricted to the ER. The expression of this novel FISP splice variant is up-regulated under ER stress in normal cells *in vivo*. In addition, FISP-sp dimerizes with FISP and blocks its secretion. Overexpression of FISP-sp reduces FISP-induced growth inhibition and apoptosis in tumor cells. Our results suggest that a novel splicing variant of mouse IL-24, FISP-sp, plays an important role in reducing the FISP-induced ER stress response *in vivo*.

EXPERIMENTAL PROCEDURES

RNA Isolation—Total RNA was isolated from cells using TRI Reagent® (Molecular Research Center) according to the manufacturer's instructions. The cDNA was synthesized from 1 μg of RNA by reverse transcription using an iScript cDNA synthesis kit (Promega), according to the manufacturer's instructions.

Quantitative Real Time PCR—A total of 50 ng of cDNA was used for quantitative real time PCR, following the manufacturer's protocol. Primers specific to FISP and FISP-sp are listed in Table 1. Primers for used analysis of GADD genes are as follows: GADD34 (forward) 5′-GAC CCC TCC AAC TCT CCT TC-3′ and (reverse) 5′-CTT CCT CAG CCT CAG CAT TC-3′; GADD45α (forward) 5′-TGG TGA CGA ACC CAC ATT CAT-3′ and (reverse) 5′-ACC CAC TGA TCC ATG TAG CGA C-3′; GADD153 (forward) 5′-ACA GAG GTC ACA CGC ACA TC-3′ and (reverse) 5′-GGG CAC TGA CCA CTC TGT TT-3′. The primer pair for mouse L32, used as a control, was (forward) 5′-GCC CAA GAT CGT CAA AAA GA-3′ and (reverse) 5′-ATT GTG GAC CAG GAA CTT GC-3′. Primers were designed to span the intron-exon borders, to allow amplified cDNA to be distinguished from genomic DNA. Quantitative real time PCR using a thermocycler (Bio-Rad) was carried out in a 20-μl reaction mixture containing SYBR Green I master mix (Takara) and 10 pM (each) PCR primers. Samples were denatured at 95 °C for 5 min and were then subjected to 40 cycles of 95 °C for 30 s, 60 °C for 15 s, and 72 °C for 30 s. The final extension was for 5 min at 72 °C. The authenticity of the PCR products was confirmed by melting curve analysis. The Opticon Monitor software package 2.0 was used for detection of fluorescent signals and for T_m calculations. The PCR-amplified products were electrophoresed in 2% agarose gels and stained with ethidium bromide.

Plasmid Constructs—The full-length mIL-24/FISP gene was amplified from a mouse Th2 D10 cell cDNA library with gene-specific primers incorporating KpnI restriction sites as follows: FISP forward (5′-CGG GGT ACC ATG CTG ACT GAG CCT GCC C-3′) and reverse (5′-CGG GGT ACC GAG ATG GTA GAA TTT CTG CAT CC-3′); FISP-sp forward (5′-CGG GGT ACC ATG CTG ACT GAG CCT GCC C-3′) and reverse (5′-CGG GGT ACC CTG GGC TGT AGT TGT GAC AT-3′). The reverse primer was designed to delete the stop codon. The PCR products were purified and inserted into pcDNA3.1/C-terminal HA, pcDNA3.1 (+) Myc-His, and pEGFP-N3, using the KpnI site of these vectors. The primer positions are based on the mIL-24/FISP sequence, GenBank™ accession number AF333251.

Cell Lines and Cell Culture—HeLa (human cervical cancer cell line), B16F10.9 (mouse melanoma cell line), NIH3T3 (mouse embryonic fibroblast), HEK293 (human embryonic kidney), COS-7 (African green monkey, kidney), and EL-4 (mouse T cell lymphoma) cells were maintained and grown in Dulbecco's modified Eagle's medium supplemented with 10% fetal bovine serum (Hyclone) and 1% penicillin/streptomycin. The murine Th2 D10 clone (D10.G4.1) was maintained as described previously (16). $CD4^+$ T cells were purified from spleen and lymph nodes of AKR mice by positive selection with anti-CD4 magnetic beads (Dynal) and differentiated under Th2 conditions according to a standard protocol (17, 18). D10 and primary Th2 cells were stimulated for 4 h with 1 μM ionomycin plus 10 nM PMA. All cultures were maintained at 37 °C in a humidified 5% CO_2 atmosphere.

Transient Transfection and Reporter Assay—Transient transfections in HEK293 cells were carried out using LipofectAMINE 2000 (Invitrogen) according to the manufacturer's instructions. To analyze whether FISP is degraded via the proteasome, and to prevent proteasomic degradation, HEK293 cells were treated with 10 μM MG132 (Sigma), a proteasome inhibitor, beginning 24 h after transfection for 12 h. For transfection into EL-4 cells, Metafectene (Biontex) was used according to the manufacturer's instructions. For the transfection of B16F10.9, HeLa, and NIH3T3 cells, the cells were washed twice with serum-free medium and resuspended in Hypo-osmolar Electroporation Buffer (Eppendorf), at a concentration of 3×10^6 cells/ml. Aliquots of the cell suspension (400 μl) were transferred into electroporation cuvettes (2-mm gap width). Cells were electroporated with 2 μg of DNA using a Multiporator® (Eppendorf), according to the manufacturer's instructions. To inhibit *N*-glycosylation and induce ER stress, cells were treated for 4 h with the ER stress inducer tunicamycin (250 ng/ml), beginning 20 h after transfection, for 6 h (19). Transient transfections in mouse primary Th2 cells were carried out using Amaxa Nucleofecter Technology (Amaxa), according to manufacturers' instructions. Primary Th2 cells (in aliquots of 2×10^6) were transfected with 4 μg of pXPG vector (20) alone or with FISP-Luc, FISP-sp-Luc, or screening-Luc (+29-SP-ΔATG-frame-3-LUC). Six hours after transfection, cells were stimulated with 1 μM ionomycin plus 10 nM PMA for 2 h and were either left untreated or were further treated with tunicamycin for 4 h. To assess luciferase activity, cells were collected, and lysates were analyzed using the dual luciferase assay system (Promega). Co-transfection of 100 ng of the pRL-TK vector (Promega) was used to normalize transfection efficiency, by measuring *Renilla* luciferase activity.

Western Blot and Immunoprecipitation Analysis—For Western blots, HEK293 cells were harvested and washed in cold phosphate-buffered saline solution (PBS). Subsequently, cells were lysed on ice in modified RIPA buffer containing 1% Nonidet P-40, 50 mM Tris-HCl (pH 7.4), 0.25% sodium deoxycholate, 150 mM NaCl, 10 mM NaF, 1 mM Na_3VO_4, 10 μg/μl

leupeptin, 1 μg/μl pepstatin, 10 μg/μl aprotinin, and 1 mM phenylmethylsulfonyl fluoride. Protein concentrations were determined by the Bradford method (Bio-Rad). Aliquots containing 30–100 μg of total protein were resolved by SDS-PAGE, using 10–12% polyacrylamide gels, and were transferred to a nitrocellulose membrane (Protran). To detect the secreted forms of protein, cells were cultured for 12 h in serum-free DMEM after 12 h of transfection. Using a Centriprep device with an Ultracel YM-3 (3,000 nominal molecular weight limit) membrane (Millipore), the collected medium (10 ml) was concentrated into 100 μl. To the concentrated supernatant was added 900 μl of ice-cold 100% acetone, and the protein was left to precipitate for 12 h. Protein concentrations were determined by the Bradford method (Bio-Rad), and 30 μg of total protein was subjected to SDS-PAGE. The following antibodies were employed to detect proteins: anti-HA.11 monoclonal (Covance Research Products), anti-Myc monoclonal, and anti-GFP monoclonal (Molecular Probes), anti-ubiquitin (Santa Cruz Biotechnology), anti-caspase (Abcam), anti-KDEL to detect GRP-78 and GRP-94 (glucose-regulated protein 78 and 94) (StressGen), anti-calreticulin (Abcam), and anti-PDI (Santa Cruz Biotechnology). Anti-β-actin monoclonal (Santa Cruz Biotechnology) and anti-glyceraldehyde-3-phosphate dehydrogenase (Lab Frontier) antibodies were used for loading controls. For immunoprecipitation analysis, HEK293 cells were harvested in PBS and incubated in 1 ml of lysis buffer (10 mM Tris-HCl, 20 mM EDTA, 10 mM NaCl, 0.1 mM phenylmethylsulfonyl fluoride, 10 μg/μl leupeptin, 1 μg/μl pepstatin, 10 μg/μl aprotinin) for 30 min on a rotary shaker at 4 °C. After centrifugation at 15,000 $\times$ *g* for 30 min at 4 °C, supernatants were incubated with 10 μl of 70% protein A-agarose at 4 °C for 1 h to eliminate nonspecific interactions. Samples were centrifuged and mixed with anti-Myc and anti-HA monoclonal antibodies (Molecular Probes) and rotated overnight at 4 °C. Immunocomplexes were precipitated with 25 μl of 50% protein A-agarose for 2 h. The immunoprecipitates were washed very gently with the immunoprecipitation buffer three times, resuspended in 50 μl of 10 mM Tris-HCl (pH 8.0) containing 1 mM EDTA, resolved by SDS-PAGE, and transferred to nitrocellulose membranes. Membranes were blocked with 5% low fat dry milk in Buffer A (25 mM Tris, 0.15 M NaCl, 0.1% Tween 20 (pH 7.3)) for 1 h at room temperature. The membranes were immunoblotted using the anti-HA.11 monoclonal (Covance Research Products) and anti-Myc antibodies for co-immunoprecipitation and the anti-ubiquitin (Santa Cruz Biotechnology) antibody for the ubiquitination study in 10 ml of Buffer A containing 2% milk for 2 h at room temperature. After washing with Buffer A, the membranes were incubated with mouse IgG TrueBlot™ at a dilution of 1:1000 in buffer containing 2% milk, for 1 h at room temperature. Membranes were washed with Buffer A, developed with ECL reagent (Amersham Biosciences), and exposed to film. For mass spectrometric analysis, immunoprecipitated samples were resolved by SDS-PAGE and silver-stained, and the required bands were cut out of the gel and used for further analysis.

Digestion of Samples for Micro-LC/LC-MS/MS Analysis—The samples were diluted 5-fold with 50 mM ammonium bicarbonate (pH 8.0) and 8 M urea, then reduced by adding tris(2-carboxyethyl)phosphine hydrochloride at room temperature for 30 min, and then carboxy-amidomethylated in 10 mM iodoacetamide at room temperature for 30 min in the dark. Endoproteinase Lys-C (Promega) was added to a final substrate:enzyme ratio of 100:1 and incubated at 37 °C for 12 h. The Lys-C-digested solution was diluted 4-fold with 50 mM ammonium bicarbonate (pH 8.0) followed by the addition of $CaCl_2$ to 2 mM. Modified trypsin (Promega) was added to a final substrate:enzyme ratio of 100:1. The trypsin digestion was performed by incubating at 37 °C for 14 h.

Micro-LC/LC-MS/MS Analysis—A single-phase microcapillary column was constructed with 100-mm inner diameter fused silica capillary tubing pulled to a 5-mm inner diameter tip using a CO_2 laser puller (Sutter Instruments, P-2000). The capillary column was packed sequentially with 7.5 cm of 5-mm inner diameter Polaris C18-A (Metachem), 4.5 cm of 5-mm inner diameter Partisphere strong cation exchange (Whatman), followed by another 3.5 cm of Polaris C18-A, using a homemade high pressure column loader. The columns were equilibrated with 5% CAN and 0.1% formic acid solution, and 10–25 mg of protein digests were directly loaded onto the capillary column. The buffer solutions used to separate protein digests were Buffer A (5% ACN and 0.1% formic acid), Buffer B (80% ACN and 0.1% formic acid), and Buffer C (500 mM ammonium acetate, 5% ACN and 0.1% formic acid). Six steps of SCX/RPLC peptide separation were performed. The first step of 120 min consisted of a 95-min gradient from 0 to 100% Buffer B and a 25-min hold at 100% Buffer B. The next five steps of 120 min each were with 55% Buffer B from 15 to 120 min. The Buffer C percentage in step 2 was 5% from 10 to 15 min, and in steps 3–6 were 10, 25, 50, and 100%, respectively, from 5 to 9 min. Peptides eluted from the capillary column were electrosprayed into an LCQ Deca XP Plus IT mass spectrometer (Thermo Finnigan) with the application of a distal 2.4-kV spray voltage. A cycle of one full scan (400–1400 *m*/*z*) followed by three data-dependent MS/MS scans at a 35% normalized collision energy was repeated throughout the LC separation. Bioworks (version 3.1) was used to filter the search results, and the following X_{corr} values were applied to the variously charged peptides as follows: 1.8 for singly charged peptides, 2.2 for doubly charged peptides, and 3.2 for triply charged peptides.

Immunocytochemistry—Both COS-7 and HeLa cells were fixed in PBS containing 4% formaldehyde and 4% sucrose for 15 min and permeabilized for 5 min in PBS containing 0.25% Triton X-100. Samples were blocked in PBS containing 10% BSA at 37 °C for 30 min and then incubated in PBS containing the primary antibodies and 3% BSA for 2 h at 37 °C or overnight at 4 °C. The samples were washed six times with PBS and incubated in PBS containing the secondary antibodies and 3% BSA for 45 min at 37 °C. For Golgi staining, cells were washed six times in PBS and then incubated in PBS/Hanks' balanced salt solution containing Golgi-BODIPY TR Ceramide (Molecular Probes) for 1 h at room temperature. Coverslips were mounted on a glass slide, and fluorescence images were acquired using an Olympus IX71 microscope equipped with a $\times$40 N.A. 1.0 or $\times$60 N.A. 1.4 oil lens and a CoolSNAP-Hq CCD camera (Roper Scientific) driven by MetaMorph (Universal Imaging Corporation) imaging software. Light from a mercury lamp was shut-

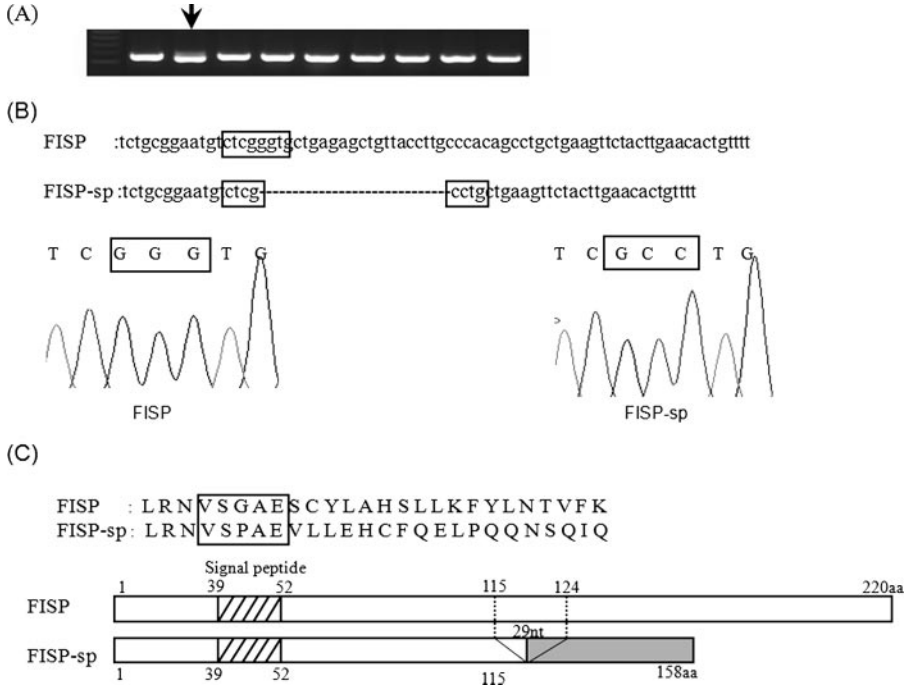

FIGURE 1. **Cloning of a novel FISP splicing variant, FISP-sp.** *A,* splicing variant of FISP, marked with an *arrow*, was cloned from a D10 cell cDNA library. The difference in the length of FISP-sp and FISP transcripts was confirmed by PCR. *B,* DNA sequence alignment of FISP and FISP-sp shows that FISP-sp lacks 29 bp from the 5′-end of FISP exon 4. *Boxed regions* indicate the site of alternative splicing in FISP. *Boxed nucleotide* sequences correspond to the sequencing histogram of FISP and FISP-sp. *C,* FISP and FISP-sp amino acid sequences are identical at the N-terminal region but are different at the C-terminal region, beginning at the *boxed area*, because of a frameshift caused by splicing. Schematic representations of FISP and FISP-sp peptide structures are shown *below* the amino acid sequence.

tered using a VMM1 Uniblitz shutter (Vincent Associates). Analysis and quantification of data were performed using MetaMorph software and Sigmaplot, and data were presented as mean ± S.E. Primary antibodies were as follows: anti-HA (Roche Applied Science), anti-His (Santa Cruz Biotechnology), and anti-PDI (Molecular Probes). Secondary antibodies were as follows: Oregon Green-conjugated goat anti-rabbit (Molecular Probes), Oregon Green-conjugated goat anti-mouse (Molecular Probes), Texas Red-conjugated goat anti-rat (Molecular Probes), and Texas Red-conjugated goat anti-mouse (Molecular Probes).

Cell Growth and Cell Cycle Analysis—Cell growth analysis experiments were conducted with exponentially, asynchronously growing cells. B16F10.9 mouse melanoma cells were transfected with vector alone, FISP-myc, FISP-sp-HA alone, or with combinations of vectors. Cell counts were determined using a hemocytometer 24, 48, and 72 h post-transfection. For the assessment of cytotoxicity in response to the addition of the proteasome inhibitor MG132, HEK293 cells were treated with increasing concentrations of MG132 (0, 5, 10, 15, and 20 μM) for 12 h. Cell viability was assessed by trypan blue dye exclusion. For cell cycle analysis, cells were harvested, washed in PBS, and fixed overnight at −20 °C in 70% ethanol. The cells were treated with RNase A (1 mg/ml) at 37 °C for 30 min and then with propidium iodide (50 μg/ml) (Sigma). The cell cycle was analyzed using an EXPO32 ADC XL4 Color (Beckman Coulter) flow cytometer, and data were analyzed with EXPO32 ADC analysis software (Beckman Coulter).

Hoechst Staining—B16F10.9 cells were transferred to 6-well plates after electroporation with a clean slide and incubated at 37 °C in humidified 5% CO_2 for 48 h. Cells were washed twice with cold PBS (pH 7.2) and stained with 0.1 μg/ml Hoechst 34580 (Invitrogen) or propidium iodide (Sigma) at 37 °C for 30 min. Nuclear morphology was observed using a fluorescence microscope (Olympus).

DNA Fragmentation Assay—Nucleosomal DNA degradation was analyzed as described previously (21) with minor modifications. Briefly, B16F10.9 mouse melanoma cells were transfected by electroporation with mock vector, FISP, or FISP-sp or were co-transfected and were seeded in 6-well culture dishes. 48 and 72 h post-transfection, cells were harvested (with trypsinization) and then lysed in a solution containing 100 mM NaCl, 10 mM Tris (pH 7.4), 25 mM EDTA, and 0.5% SDS. After centrifugation, the supernatants were incubated with 300 μg/ml proteinase K for 5 h at 65 °C and extracted with phenol/chloroform. The aqueous layer was treated with 0.1 volume of 3 M sodium acetate; the DNA was precipitated with 2.5 volumes of 95% ethanol. After treatment with 100 mg/ml RNase A for 1 h at 37 °C, the sample was electrophoresed on a 2% agarose gel at 50 V for 2 h and then stained with ethidium bromide.

RESULTS

Identification of FISP-sp, a Novel Splicing Variant of Mouse IL-24/FISP—Mouse IL-24/FISP is selectively expressed in Th2 cells (6). During cloning of the mIL-24/*FISP* gene into a mammalian expression vector, we identified a novel splicing variant of FISP, namely FISP-sp. Initially, total RNA and cDNA were prepared from D10 cells (mouse Th2-type clone) and stimulated with PMA and ionomycin for 4 h. The cDNA was PCR-amplified using primer sets spanning the coding region of the FISP gene. In addition to the FISP-coding sequence fragment, a slightly smaller sized FISP-coding fragment, FISP-sp, was identified and cloned (Fig. 1*A*). Sequencing analysis revealed that FISP-sp lacks 29 bp from the 5′-end of the full-length FISP exon 4 gene (Fig. 1*B*). This alternative splicing occurs at an A(G/G)T site, which is the splice site sequence comprising the major class of AG-GT introns. The entire FISP-sp sequence was deposited in GenBank™ accession number DQ401033. Removal of 29 bp by splicing activity leads to a frameshift, starting at amino acid 116, and a subsequent translation termination because of a newly generated stop codon. The predicted primary structure of FISP-sp contains 158 amino acids, instead of 220 amino acids as in FISP. FISP-sp and FISP share identical amino acid

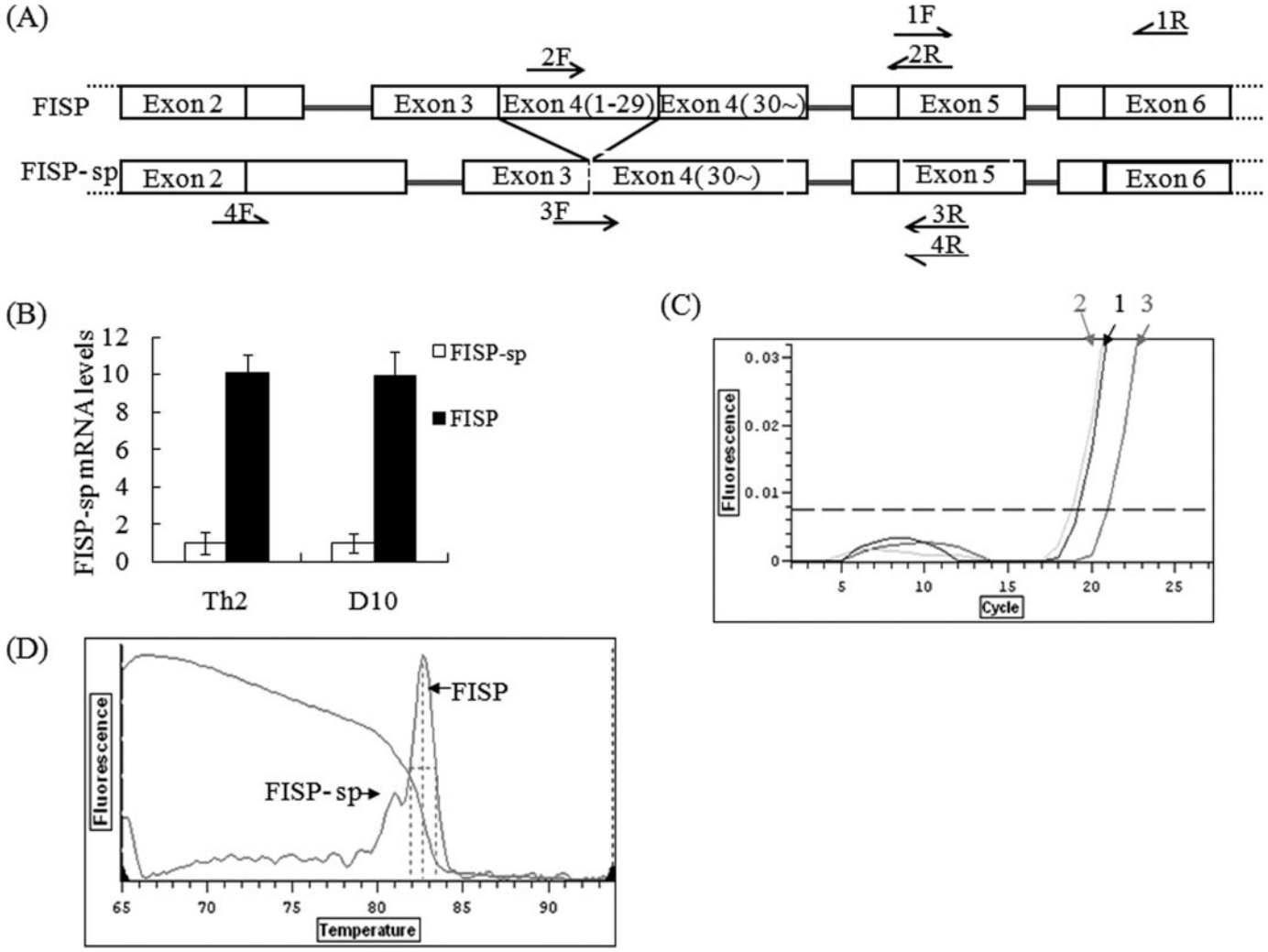

FIGURE 2. **Relative mRNA levels of FISP and FISP-sp in Th2 cells.** The mRNA expression levels of FISP and FISP-sp were analyzed by quantitative real time PCR in Th2 D10 cells and in 5-day differentiated primary Th2 cells. In quantitative real time PCR amplification, the normalized reporter signal represents the fluorescence changes adjusted to base-line levels before amplification and the threshold cycle (*Ct*) of amplified products. *A,* designed primer sets are as follows: common to FISP and FISP-sp (set 1), FISP (set 2), FISP-sp (set 3), and specific for both FISP and FISP-sp but yielding amplicons of different sizes because of splicing of 29 bases (set 4). *B,* ratio of FISP to FISP-sp mRNA was shown to be ~10:1 in D10 and Th2 cells. *C,* threshold cycle of amplified products, which were amplified using primer sets 1, 2, and 3. *D,* melting curve graph for PCR products amplified by primer set 4 demonstrates the presence of two different species of amplified PCR products. *Arrows* indicate the relative peaks of FISP and FISP-sp.

sequences in their first 115 N-terminal amino acids, but FISP-sp has a completely different sequence in its 43 C-terminal amino acids, derived from the frame-shifted translation of the FISP ORF 3 (Fig. 1*C*).

Quantitation of FISP-sp Expression Levels in T Cells—To determine the relative expression levels of FISP-sp and FISP, we performed quantitative real time RT-PCR with four sets of primer pairs (Fig. 2*A*, and Table 1). Primers were designed to detect sequences that were (i) common to FISP and FISP-sp (set 1; same amplicon size), (ii) FISP-specific (set 2), (iii) FISP-sp-specific (set 3; starting from just before the splicing site and extending to exon 4, and (iv) common to FISP and FISP-sp but yielding different amplicon sizes because of splicing of 29 bases (set 4). As shown in Fig. 2*D*, RT-PCR using primer set 4 resulted in PCR products of two different amplicons, confirmed by melting curve analysis. This result suggests that two transcript isoforms with different sizes exist in the T cell cDNA library. FISP-sp mRNA levels were found to be about 10% of total FISP mRNA, in both D10 cells (mouse Th2 clone) and primary Th2 cells (Fig. 2, *B* and *C*). The specificity of the FISP and FISP-sp primer sets was confirmed by DNA sequencing and melting curve analysis (data not shown).

TABLE 1
Mouse IL-24/FISP mRNA primer sets for real time PCR

Primer set 1 (Common)	Forward	5′-GCCCAGTAAGGACAATTCCA-3′
	Reverse	5′-ATTTCTGCATCCAGGTCAGG-3′
Primer set 2 (FISP-specific)	Forward	5′-AGCTGTTACCTTGCCCACA-3′
	Reverse	5′-GCATGGAATTGTCCTTACTGGGCT-3′
Primer set 3 (FISP-sp-specific)	Forward	5′-GCCCAGTAAGGACAATTCCA-3′
	Reverse	5′-GCATGGAATTGTCCTTACTGGGCT-3′
Primer set 4 (common but different amplicon size)	Forward	5′-CTCAGGATGACATCACAAGC-3′
	Reverse	5′-GCATGGAATTGTCCTTACTGGGCT-3′
Primer set 5 (transfected FISP-specific)	Forward	5′-GCCCAGTAAGGACAATTCCA-3′
	Reverse	5′-TGAAGTTGTTGGCCAGAGTG-3′
Primer set 6 (transfected FISP-sp-specific)	Forward	5′-GCCCAGTAAGGACAATTCCA-3′
	Reverse	5′-TGAAGTTGTTGGCCAGAGTG-3′

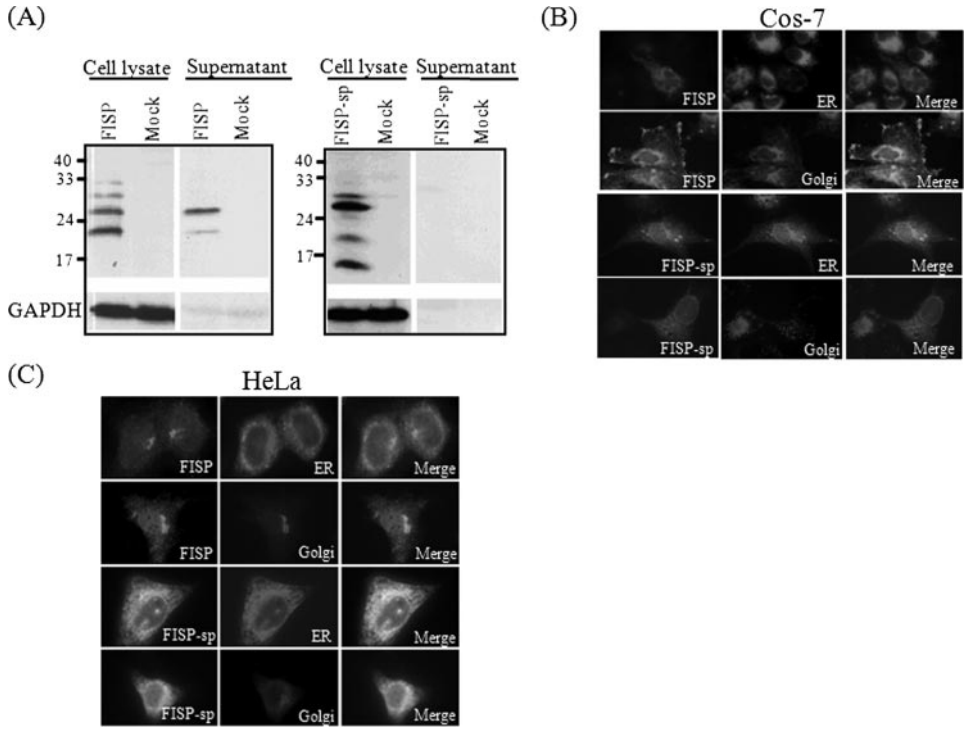

FIGURE 3. **FISP-sp is not secreted but is specifically localized in the ER.** *A,* protein expression of FISP and FISP-sp. HEK293 cells were transiently transfected with 3′-Myc/His-tagged FISP (FISP-Myc/His), 3′-HA-tagged FISP-sp (FISP-sp-HA), or empty vectors (pcDNA 3.1 Myc-His A, and pcDNA 3.1-HA). Protein lysates were collected from cells after transfection with FISP-Myc/His, FISP-sp-HA, or vector alone. Samples (30 μg) were used for Western blot analysis using mouse anti-Myc and anti-HA antibodies. To detect the secreted forms of FISP and FISP-sp protein, cells were cultured for 12 h in serum-free DMEM. Conditioned medium was collected and concentrated 60-fold. A volume of 20 μl conditioned medium was subjected to SDS-PAGE. Glyceraldehyde-3-phosphate dehydrogenase (*GAPDH*) was used as loading control. *B,* subcellular localization of FISP and FISP-sp in COS-7 cells. Protein localization was analyzed by immunocytochemistry. FISP was detected using anti-His or anti-Myc antibodies, and FISP-sp was detected using an anti-HA antibody. The Golgi and ER were visualized using Golgi-BODIPY TR ceramide and an anti-PDI antibody. Images of different cellular compartments exhibiting FISP and FISP-sp staining were merged. FISP protein staining partially overlapped with ER and Golgi apparatus staining. However, staining of FISP-sp protein matched exactly with ER staining and was not detected in the Golgi apparatus. *C,* subcellular localization of FISP and FISP-sp in HeLa cells.

FISP-sp Is Not Secreted but Is Specifically Localized in ER—The predicted ORF of FISP and FISP-sp codes 220 and 158 amino acids, respectively (Fig. 1*C*). Homology between the FISP-sp protein and full-length FISP is limited to the first 115 amino acids of the N-terminal region. Because FISP-sp contains the same signaling peptides and cleavage sites as FISP (Fig. 1*C*), we tested whether, like FISP, FISP-sp is secreted. To assess protein secretion, the coding sequences of FISP and FISP-sp were fused to 3′-Myc/His-and 3′-HA-tagged vectors, respectively. These constructs were transiently transfected into HEK293 cells, and the cell lysates and supernatant (serum-free DMEM) were subjected to Western blot analysis 24 h post-transfection. The results revealed that although FISP-sp shares N-terminal signaling peptides, it is not secreted (there was no signal in the supernatant fraction) and is exclusively isolated in the cell pellet (Fig. 3*A*). Next, the subcellular localization of FISP and FISP-sp was analyzed in transiently transfected COS-7 cells, 24 h post-transfection. Expressed FISP (FISP-Myc/His) and FISP-sp (FISP-sp-HA) were detected using specific antibodies against their respective C-terminal immunocytochemistry tags. FISP protein staining was observed in extra-nuclear regions of individual cells (Fig. 3*B*). Although there was a light background of cytoplasmic staining, FISP protein staining patterns partially overlapped with the ER and Golgi. In addition, staining of a membrane-bound form of FISP was observed. However, the FISP-sp staining pattern overlapped exactly and exclusively with the ER (Fig. 3*B*). FISP localization varied slightly from that of human IL-24/MDA-7, which specifically resides in the ER (22, 23). We also saw similar subcellular localization patterns for FISP and FISP-sp in HeLa, a human cervical cancer cell line (Fig. 3*C*).

FISP-sp Antagonizes FISP-induced Inhibition of Cell Growth and Apoptosis—MDA-7/IL-24 is known to induce apoptosis in tumor cells and shows growth-suppressive activity in a spectrum of human cancer cells both *in vitro* and *in vivo* (9, 12–14, 24–27). Recently, a report by Chen *et al.* (14) showed that mouse IL-24/FISP mediates tumor suppression in mice, but the mechanism of suppression remains unclear. Until now, little information has been available on the role of MDA-7/IL-24/FISP splicing variants. To understand the biological role of FISP-sp in the context of mIL-24/FISP-induced inhibition of cell growth, FISP, FISP-sp, or FISP and FISP-sp together were transfected into the mouse melanoma cell line B16F10.9. Cell viability was monitored 24, 48, and 72 h post-transfection by trypan blue dye exclusion. Overexpression of FISP led to cell growth inhibition at 24 h post-transfection, and this inhibition was profoundly increased at 72 h (Fig. 4*A*) compared with mock vector-transfected cells. This inhibition was comparable with the growth inhibition induced by tunicamycin. However, FISP-sp did not induce cell growth inhibition in comparison with vector alone. Upon co-transfection of FISP and FISP-sp, cell growth was rescued in B16F10.9 cells, suggesting that FISP-sp may antagonize FISP-mediated inhibition of cell growth (Fig. 4*A*). Because IL-24 is a potent cancer cell-specific apoptosis-inducing cytokine, we tested whether this growth inhibition by FISP is apoptosis-related. Apoptosis is an active process of self-destruction associated with profound structural changes, including morphological alteration, increased membrane permeability, and nuclear collapse, characterized by chromatin condensation and DNA fragmentation (28, 29). Because growth inhibition by FISP was maximal at 72 h post-transfection, we began by analyzing the morphological characteristics of B16F10.9 cells transfected with mock vector, FISP, FISP-sp alone, or FISP + FISP-sp together. Microscopic examination revealed that FISP-transfected cells featured a more prominent nucleus and were in the later morphological stages of apoptosis (*i.e.* severe mem-

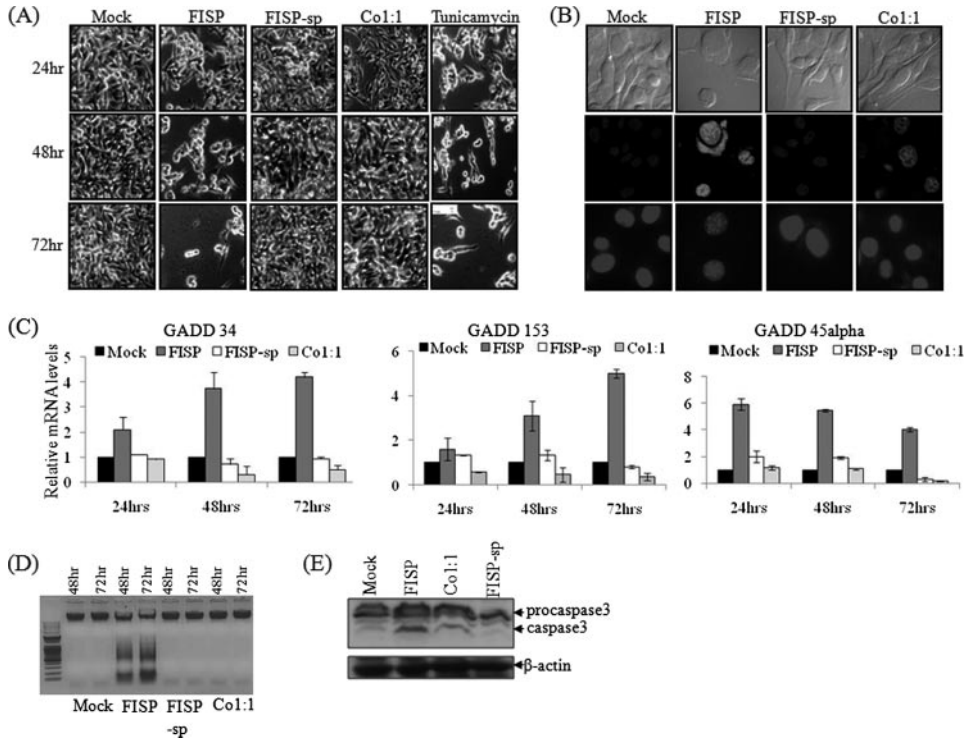

FIGURE 4. **FISP-sp inhibits FISP-induced cell growth inhibition and apoptosis.** *A,* effect of the control vector, FISP, FISP-sp, and FISP + FISP-sp upon the growth of B16F10.9 cells, analyzed 24, 48, and 72 h post-transfection. *B,* apoptotic changes in B16F10.9 cells were analyzed after transfection with mock vector, FISP, FISP-sp, or FISP + FISP-sp. At 72 h post-transfection, photomicrographs were taken of adherent cells in each sample (*upper panel*). The cells were then washed and stained with 0.1 μg/ml Hoechst 34580 (Invitrogen) or propidium iodide (Sigma). The slides were then examined by fluorescence microscopy and photographed. Cells showing signs of apoptosis (fragmented nuclei) and membrane blebbing are shown using Hoechst and propidium iodide treatment, respectively (*bottom* and *middle panels*, respectively). *C,* overexpression of FISP induces expression of the GADD family of genes in B16F10.9 melanoma cells, in a time-dependent manner. Total RNA was extracted, and real time PCR analysis was performed using specific primers. All of the GADD genes examined were found to be up-regulated in the FISP-transfected samples but not in the samples transfected with FISP-sp or FISP + FISP-sp. *D,* B16F10.9 cells were transfected with either mock vector, FISP, FISP-sp, or FISP + FISP-sp. At 48 and 72 h post-transfection, DNA was extracted from the cells, and fragmentation was analyzed. *E,* FISP activates caspase-3 in tumor cells. Activation of procaspase-3 is indicated by the generation of its cleavage products, as observed in FISP-transfected B16F10.9 mouse melanoma cells, but not in FISP-sp-treated cells. β-Actin was used as a loading control.

brane blebbing; Fig. 4*B*, *upper panel*), whereas FISP-sp-transfected cells had intact morphological shapes. Nuclear condensation and DNA fragmentation were detected by Hoechst staining and fluorescence microscopy in FISP-transfected cells (Fig. 4*B*, *bottom panel*). Unlike FISP, FISP-sp did not induce any apoptotic characteristics and upon co-transfection decreased the apoptotic effects of FISP. Similar effects were observed following propidium iodide staining (Fig. 4*B*, *middle panel*). When FISP and FISP-sp were co-transfected, the apoptotic characteristics induced by FISP were greatly reduced (Fig. 4*B*). Flow cytometric analysis was performed after staining cells with the vital dye propidium iodide. FISP overexpression increased the level of cell death observed in B16F10.9 cells 24 h after transfection (sub G_0/G_1 phase) by ~24% (supplemental Fig. 1). However, FISP overexpression did not induce significant levels of cell death in the non-cancer cell line, NIH3T3 cells. Compared with FISP, FISP-sp alone did not induce a significant amount of cell death. To examine whether FISP-sp affects IL-24/FISP-mediated cell death in cancer cells, B16F10.9 cells were co-transfected with FISP and FISP-sp, and the level of FISP-mediated cell death was found to be reduced from 24.26 to 6.47%, raising the possibility that FISP-sp inhibits FISP-induced cell death in tumor cells (supplemental Fig. 1).

A previous report shows that the *GADD* family genes, namely *GADD34*, *GADD45-α*, and *GADD153*, were induced upon adenoviral expression of MDA-7 (30). Hence, we investigated whether FISP overexpression up-regulates these genes, and what the role of FISP-sp might be in this context. B16F10.9 melanoma cells were transfected with mock vector, FISP, FISP-sp, or FISP + FISP-sp. Total RNA was extracted, and the mRNA expression of the GADD family of genes was analyzed using real time PCR. As shown in Fig. 4*C*, the expression levels of GADD34 and GADD153 gradually increased as apoptosis progressed in FISP-transfected cells. At 24 h their levels were low, but expression increased progressively until 72 h. The level of GADD45-α was significantly increased even after 24 h of FISP transfection. However, FISP-sp alone did not induce the expression GADD34, GADD153 or GADD45-α. Interestingly, co-transfection of FISP-sp with FISP significantly reduced the expression levels of the GADD family genes examined. A previous report shows that MDA-7/IL-24 overexpression up-regulates ER stress markers like BiP/GRP78, GRP94, calreticulin, XBP1, and eIF2α (31).We further evaluated the expression of ER chaperones whose up-regulation frequently correlates with UPR resulting from ER stress. We overexpressed FISP, FISP-sp, or FISP + FISP-sp in HeLa and B16F10.9 cells. 48 h post-transfection expression of ER stress-response genes was analyzed. BiP/GRP78, GRP94, calreticulin, and PDI were specifically up-regulated in B16F10.9 and HeLa cells upon FISP transfection comparable with tunicamycin-treated cells (supplemental Fig. 2).This result was in accordance to the previous report (31). However, FISP-sp did not up-regulate any of these proteins when transfected alone or when co-transfected with FISP, and it further blocked their up-regulation (supplemental Fig. 2). These results further substantiate our finding that FISP-sp indeed blocks FISP-induced apoptosis in cancer cells.

To further test whether FISP induces apoptosis in cancer cells, we performed a DNA fragmentation assay. B16F10.9 cells were transfected with mock DNA, FISP, FISP-sp, or FISP + FISP-sp. To detect internucleosomal DNA fragmentation (DNA laddering), DNA extracted from the transfected cells was

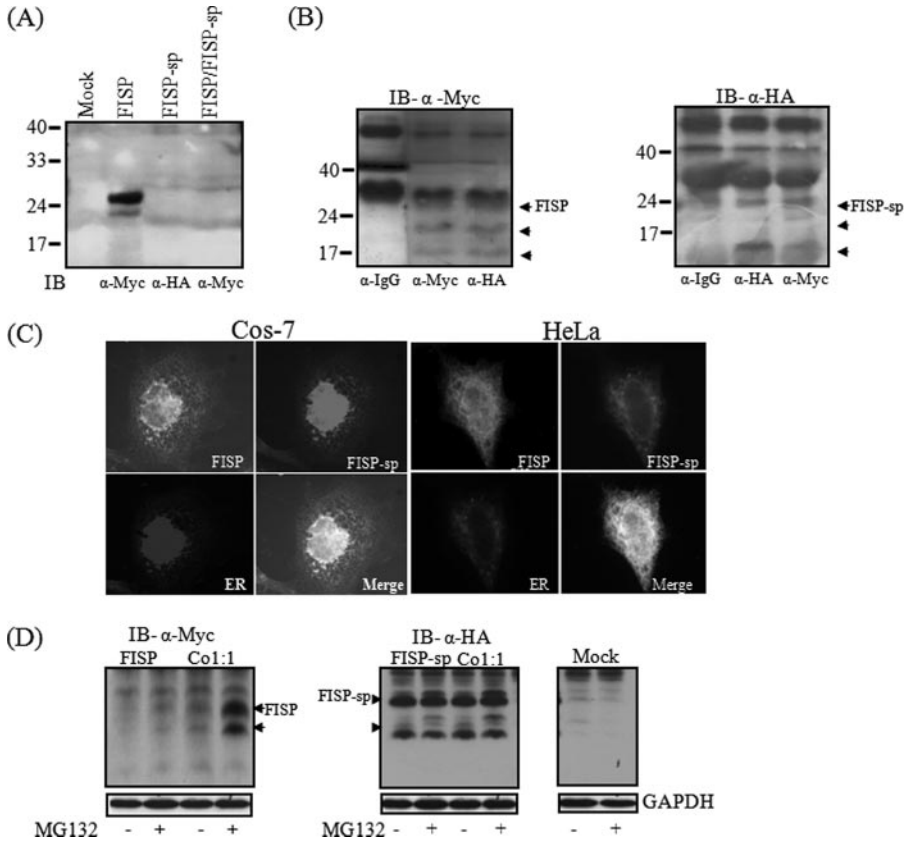

FIGURE 5. **Physical interaction of FISP and FISP-sp.** *A,* FISP-sp blocks FISP secretion. HEK293 cells were transiently transfected with 3′-Myc/His-tagged FISP (FISP-Myc/His) or 3′-HA-tagged FISP (FISP-HA), or their respective empty vectors (pcDNA 3.1 Myc-his A, and pcDNA 3.1-HA). To detect the secreted forms of these proteins, cells were cultured for 12 h in serum-free DMEM. Conditioned medium was collected, concentrated 100-fold, precipitated with 100% acetone, and subjected to SDS-PAGE and Western blot analysis using mouse anti-Myc and anti-HA antibodies. *IB,* immunoblot. *B,* FISP-sp physically interacts with FISP. HEK293 cells were transiently transfected with 3′-Myc/His-tagged FISP (FISP-Myc/His) or 3′-HA-tagged FISP-sp (FISP-sp-HA) expression vectors. Immunoprecipitation analysis was performed 24 h post-transfection using anti-Myc, anti-HA, or anti-IgG (control) antibodies, and the same samples were further analyzed using Western blot analysis as indicated. FISP and FISP-sp bands are indicated by *arrows*. *C,* subcellular localization of FISP and FISP-sp upon expression vector co-transfection in COS-7 and HeLa cells. Protein localization was analyzed by immunocytochemistry. FISP was detected using anti-His or anti-Myc antibodies, and FISP-sp was detected using an anti-HA antibody. The ER was visualized using an anti-PDI antibody. Images of ER compartments and FISP or FISP-sp staining were merged. The pattern of FISP protein staining overlapped exactly with that of FISP-sp staining in the ER compartment, in both in COS-7 and HeLa cells. *D,* HEK293 cells were transfected with 3′-Myc/His-tagged FISP (FISP-Myc/His) or 3′-HA-tagged FISP-sp (FISP-sp-HA), or were co-transfected with both expression vectors. MG132 (10 μM) was added to cells 24 h post-transfection or cells were left untreated. Cells were analyzed 12 h later by Western blot analysis using anti-Myc or anti-HA antibodies. Bands corresponding to FISP and FISP-sp are indicated by *arrows*.

separated by agarose gel electrophoresis. As shown in Fig. 4*D*, FISP induced significant DNA fragmentation starting at 48 h. No significant DNA fragmentation was observed at 24 h post-transfection (data not shown). As expected, FISP-sp did not induce DNA fragmentation. Co-transfection of FISP and FISP-sp inhibited FISP-mediated DNA fragmentation (Fig. 4*D*). To rule out the possibility that the results on induction of cancer-specific cell death by FISP were because of differing transfection efficiencies between the NIH3T3 and B16F10.9 cells, the relative expression levels of FISP and FISP-sp were analyzed by RT-PCR. Their expression levels were similar, regardless of cell type (supplemental Fig. 3). Because morphological changes, up-regulation of GADD genes, and increased fragmentation of DNA were observed in FISP-transfected B16F10.9 cells, the expression level of caspase-3 was also analyzed to determine whether processing of procaspase-3 to active caspase-3 might be activated by FISP. B16F10.9 cells were transfected with either mock DNA, FISP, FISP-sp, or FISP + FISP-sp. Levels of the active form of caspase-3, generated by the cleavage of procaspase-3, were increased in FISP-transfected but not in FISP-sp-transfected cells (Fig. 4*E*). Co-transfection of FISP and FISP-sp reduced the generation of caspase-3 by FISP (*3rd lane* in Fig. 4*E*). These results show that FISP inhibits cell growth and induces apoptosis in B16F10.9 cells by activating cell signaling molecules associated with apoptosis, resulting in cell death. However, these FISP-mediated effects appear to be reduced or absent when FISP is co-expressed with its splicing variant, FISP-sp. These results are in accordance with previous studies, which report that the growth-suppressive activities of IL-24/MDA-7 are restricted to melanoma cells and are not observed in normal fibroblasts or in epithelial cells (8, 30, 32). Our results suggest that FISP is a true homolog of human IL-24/MDA-7 with growth-inhibitory effects specific to cancer cells and that FISP-sp inhibits this property of FISP.

FISP-sp Heterodimerizes with FISP, Leading to Its Retention in the ER—Next, the molecular mechanism of FISP-sp-mediated inhibition of FISP function was examined. IL-24 is a tumor suppressor gene that functions as a cytokine, and it is secreted both by normal cells and by cancer cells upon adenoviral delivery (33–36). The significant bystander activity of secreted IL-24 is well documented (13, 25, 34, 37–41). A previous report suggested that a novel splice variant of IL-24, MDA-7S, decreased the secretion of human IL-24/MDA-7 in melanocytes via physical interaction (15). Hence, we attempted to determine whether FISP-sp inhibits the secretion of FISP, as FISP-sp itself is not secreted. Western blot analysis revealed that upon FISP + FISP-sp co-transfection, FISP-sp completely blocked FISP secretion (Fig. 5*A*). We next investigated whether there exists any physical interaction between FISP and FISP-sp. Following immunoprecipitation and Western blot analysis in HEK293 cells co-transfected with FISP and FISP-sp expression vectors, FISP and FISP-sp were found to interact (Fig. 5*B*). This interaction appeared to alter FISP localization, causing FISP to be localized exclusively in the ER, along with FISP-sp, both in COS-7 and HeLa cells (Fig. 5*C*).

Proteasomal Degradation of FISP upon Interaction with FISP-sp—The ubiquitin proteolytic system plays an important role in a broad array of basic cellular processes (42). The list of cellular proteins targeted by ubiquitin is growing rapidly. Among them are cell cycle regulators, tumor suppressors and growth modulators, transcriptional activators and their inhibitors, cell surface receptors, and endoplasmic reticulum proteins (43). Because co-expression of FISP and FISP-sp causes FISP to be retained in the ER, and inhibits its secretion, rendering it functionally inactive, we further queried the fate of the retained FISP protein. The possibility was investigated that inactivation of FISP might lead to its degradation via the proteasome. In cells co-transfected with FISP + FISP-sp expression vectors, treatment with the proteasome inhibitor MG132 showed increased accumulation of FISP (Fig. 5*D*), whereas there was no change in FISP levels in cells transfected only with the FISP-containing vector. FISP-sp levels did not differ significantly between samples transfected with FISP-sp alone or FISP-sp + FISP. As such, it appears that FISP is recruited to the proteasome and is possibly ubiquitinated, in the presence of expressed FISP-sp. The possible cytotoxic effect of MG132 upon HEK293 cells was investigated by treating cells with increasing concentrations of MG132 (0, 5, 10, 15, and 20 μM) for 12 h (supplemental Fig. 4). Cell viability remained greater than 90% after treatment with 10 μM MG132 for 12 h. Further analysis of whether the FISP protein was ubiquitinated was undertaken using immunoprecipitation assays. Ubiquitinated FISP was detected in FISP + FISP-sp co-transfected cell lysates between 17 and 25 kDa (supplemental Fig. 5). The 25-kDa fraction of the IL-24 protein overlapped with the light chain of immunoglobulin G and hence could not be separately distinguished. However, the intensity of the 25-kDa band in the co-transfected cells (*lane 3* of *left panel* in supplemental Fig. 5) was increased relative to that of the FISP-transfected cells (*lane 2* of *left panel* in supplemental Fig. 5), indicating the presence of ubiquitinated FISP protein with a molecular mass of ~25 kDa. Proteomic analysis was performed to identify FISP-sp/FISP-interacting proteins (supplemental Table 1). Along with the FISP and FISP-sp peptides, peptides of various proteins involved in ubiquitination were detected, including ubiquitin-activating enzyme and ubiquitin-conjugating enzyme along with other proteins having important roles in the ubiquitin-proteasome pathway (43). These results suggest that FISP is ubiquitinated and that treatment with MG132 results in its accumulation.

Expression of FISP-sp Is Increased under ER Stress—Accumulation of unfolded or misfolded proteins in the ER induces a cellular state of ER stress, which in turn induces apoptosis. ER stress is known to be involved in the pathogenesis of diverse human diseases. Recent studies have shown that the anti-tumor activity of MDA-7/IL-24 in cancer cells is associated with ER stress-mediated cytotoxicity and up-regulation of ER stress-induced GRP78/BiP expression (26, 27, 31). A report by Gupta *et al.* (23) shows that human IL-24/MDA-7 physically interacts with BiP/GRP78 through its C and F helices and induces cancer-selective apoptosis, but the exact mechanism of FISP-induced inhibition of cell growth is unclear.

Based on the findings that FISP-sp inhibits FISP-induced apoptosis and growth inhibition in tumor cells (Fig. 4), we hypothesized that FISP-sp expression could be up-regulated upon ER stress to serve as a defense mechanism, rescuing normal cells from FISP-mediated growth arrest. Vector systems were designed, to quantitatively assess the generation of FISP-sp under conditions of ER stress, by monitoring a GFP or luciferase signal. The mouse *IL-24/FISP* gene was fused to the *GFP* or *LUC* gene in such a way that the generation of functional GFP or luciferase was splicing-dependent. Shown in Fig. 5*A* are the vectors +29-SP-ΔATG-frame3-GFP and +29-SP-ΔATG-frame3-LUC, which contain the full-length IL-24/FISP gene fused into the reading frame-3 of GFP or luciferase, respectively. When mIL-24/FISP mRNA was spliced to create FISP-sp mRNA, the 3′-tagged GFP or luciferase fusion gene would be functionally expressed as FISP-sp-GFP or FISP-sp-LUC protein, respectively, because of an in-frameshift (from reading frame 1–3). However, if splicing did not occur, the 3′-tagged GFP or luciferase fusion protein would not be expressed, since translation of the frame 1-encoded protein would stop before reaching the GFP start codon. To eliminate GFP false-positive signals, the start codon of GFP was deleted by site-specific deletion mutagenesis (Fig. 6*A*).

To test whether the generation of FISP-sp is ER stress-dependent, we overexpressed the +29-SP-ΔATG-frame3-GFP and +29-SP-ΔATG-frame3-LUC vectors through transient transfection into HEK293, NIH3T3, B16F10.9, HeLa, and EL-4 cells. Analysis of HEK293 and EL-4 cells transfected with the +29-SP-ΔATG-frame3-LUC vector revealed a 1.5-fold increase in gene activity upon treatment with the ER stress inducer tunicamycin (2 μg/ml, inhibits protein *N*-glycosylation) in comparison with untreated samples, suggesting that ER stress plays a role in inducing expression of the splicing variant FISP-sp (Fig. 6*B*). NIH3T3 cells transfected with +29-SP-ΔATG-frame3-GFP showed an increase in the number of GFP-positive cells when treated with tunicamycin (2 μg/ml). The ER stress-dependent levels of GFP expression were determined by Western blot analysis using a monoclonal GFP antibody (Fig. 5*B*). Removal of 29 bp by splicing was predicted to lead to the expression of a GFP-tagged protein the same size as FISP-sp-GFP (Fig. 6*B*, *1st lane*). Indeed, as shown in Fig. 6*B*, bands corresponding to FISP-sp-GFP were detected in the *2nd* and *3rd lanes* and were notably increased by ER stress. In addition, GFP expression (27 kDa) was observed only in samples treated with tunicamycin, suggesting that generation of functional GFP was because of induction of the splicing variant in conditions of ER stress (Fig. 6*B*, *3rd lane*). Similar results were obtained in cells treated with thapsigargin (500 nM), which inhibits Ca^{2+} ATPase in the ER (data not shown).

To further confirm the above results, levels of FISP-sp mRNA were measured using quantitative real time RT-PCR with specific primer sets (primer set 5 and 6, see Table 1) for FISP and FISP-sp (Fig. 6*C* and Table 1). NIH3T3 cells were transfected with +29-SP-ΔATG-frame3-GFP or vector alone and treated with or without tunicamycin. Similarly, EL-4 cells were transfected with +29-SP-ΔATG-frame3-LUC or vector alone. Total RNA was extracted and cDNAs were synthesized, as described under "Experimental Procedures." A slight (1.8-fold) increase in FISP mRNA levels was observed under conditions of ER stress, as compared with the levels observed in

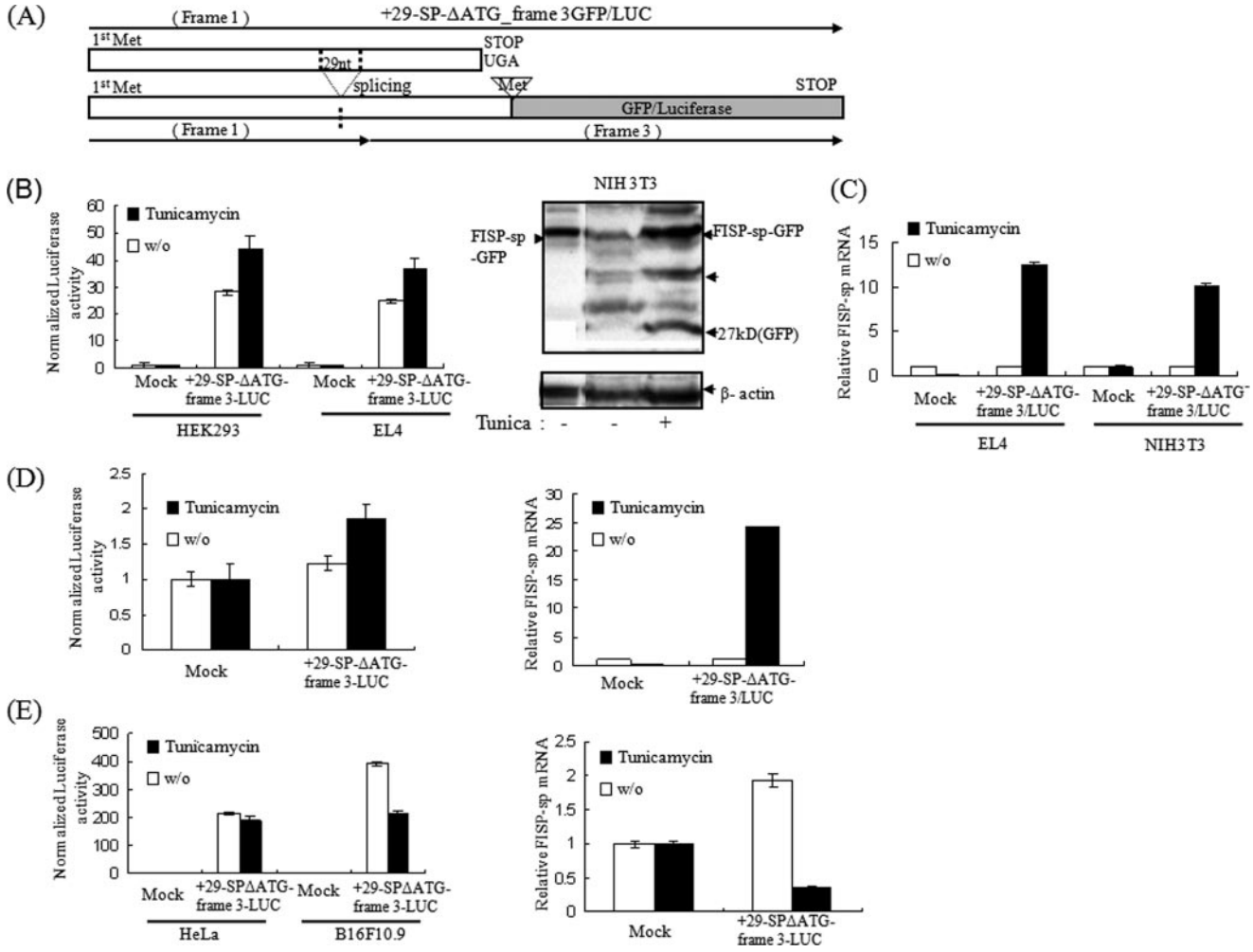

FIGURE 6. **Generation of FISP-sp under conditions of ER stress.** *A,* schematic representations of protein structures resulting from the +29-SP-ΔATG-frame3-GFP and +29-SP-ΔATG-frame3-LUC vectors. *B,* HEK293 and EL-4 cells were transfected with the +29-SP-ΔATG-frame3-LUC vector or with the pXPG vector as a control (*mock*). Higher levels of luciferase activity were observed in tunicamycin-treated samples, compared with untreated samples. NIH3T3 cells were transiently transfected with the +29-SP-ΔATG-frame3-GFP vector. Anti-GFP monoclonal antibodies were used for Western blot analysis. Bands matching the size of the expressed FISP-sp-GFP protein were more pronounced in their intensity, in cells treated with tunicamycin. *C,* cDNA from +29-SP-ΔATG-frame3-LUC or vector only. Transfected NIH3T3 and EL-4 cells left untreated or treated with tunicamycin were prepared and analyzed by quantitative real time PCR analysis. Expression levels in untreated (*w/o*) samples were assigned a value of 1. The fold change in FISP-sp expression upon tunicamycin treatment was determined by comparison of treated and untreated samples. *D,* transient transfections in mouse primary Th2 cells were carried out, and luciferase activity was analyzed. Cells were collected, and lysates were assessed using the dual luciferase assay system. Analysis of mRNA levels revealed a 25-fold increase upon induction of ER stress. Expression levels in untreated (*w/o*) samples were assigned a value of 1. The data are representative of at least two independent experiments. *E,* transient transfections in B16F10.9 and HeLa cells were performed, and analysis of luciferase activity was performed as described above. Analysis of mRNA levels revealed a 75% decrease upon induction of ER stress in B16F10.9 cells. The data are representative of at least two independent experiments.

untreated NIH3T3 cells (data not shown). However, the FISP-sp mRNA levels increased ~10- and 13-fold in tunicamycin-treated NIH3T3 and EL-4 cells, respectively, when compared with untreated cells (Fig. 6*C*). These data suggest that conditions of ER stress lead to the generation of FISP-sp and clearly demonstrate that ER stress plays a crucial role in the generation of FISP-sp in normal cells. As such, increased FISP-sp levels might be involved in rescuing cells from ER stress-induced cell death.

We further analyzed the effect of ER stress on FISP-sp synthesis in primary T cells. CD4 cells purified from mouse spleen and lymph node were differentiated *in vitro* into Th2 cells over a period of 6 days and then were transfected with +29-SP-ΔATG-frame3-LUC or mock vector. A luciferase assay revealed only a 1.5-fold increase in luciferase activity, indicating that FISP-sp was generated upon induction of ER stress in +29-SP-ΔATG-frame3-LUC-transfected cells (Fig. 6*D*). However, there was a dramatic ~25-fold enhancement in levels of FISP-sp mRNA upon induction of ER stress, whereas only basal levels of expression were observed in cells transfected with vector alone or those not receiving ER stress induction, demonstrating the strong involvement of ER stress in the generation of FISP-sp *in vivo* (Fig. 6*D*). To further test whether FISP-sp mRNA levels or splicing-dependent luciferase activity were increased in cancer cells such as B16F10.9 and HeLa cells, a luciferase assay was undertaken (Fig. 6*E*, *left*). No increase in FISP-sp levels was observed following ER stress induction in HeLa cells, whereas in B16F10.9 cells, a 40% decrease in FISP-sp levels was observed. Similarly, a 75% decrease in FISP-sp mRNA levels was observed following ER stress induction in B16F10.9 cells, with only basal levels seen in cells transfected with vector only (Fig. 6*E*, *right*). These results suggest that the

cancer cell machinery might inhibit the generation of the FISP-sp protein, thereby rendering tumor cells more susceptible to FISP-induced apoptosis.

DISCUSSION

Alternative splicing of pre-mRNA generates two or more protein isoforms from a single gene, thereby generating protein diversity. Recent studies have suggested that splicing variants play a regulatory role in controlling the function and/or activity of their full-length counterparts (44). In this study, we have identified a novel splicing variant of mouse IL-24/FISP, designated it with the name FISP-sp, and characterized its subcellular localization and biological function. Alternative splicing of 29 nucleotides at the 5′-end of exon 4 of FISP induces a frameshift and leads to premature termination of wild type mouse IL-24/FISP at amino acid 158 instead of amino acid 220. Expression of FISP-sp is increased under ER stress. Unlike FISP, FISP-sp is specifically localized in the ER and antagonizes the growth inhibition, ER stress induction, and apoptosis induced by FISP. FISP-sp physically interacts with FISP, which retains FISP in the ER, and subsequently leads to degradation of FISP by the proteasome.

Mouse IL-24/FISP is classified as an IL-10 cytokine family member (38) based on its chromosomal location, sequence, and structure homology. Like other IL-10-related cytokines, mIL-24/FISP is a secreted α-helix protein. Although its function has not yet been elucidated, it is thought that FISP might play an important role in the immune system as a cytokine. FISP-sp, the novel splicing variant identified here, loses its homology with FISP in the C terminus, a region of FISP that includes half of the IL-10 signature sequence (AHSLLKFYLNTVFKNYHSKI-AKFK) and the helix C to F domain. Unlike mIL-24/FISP, FISP-sp is not secreted and is specifically localized in the ER, suggesting that it might not function as a cytokine but rather might exert its activity in the ER in the context of FISP expression. In cells, splicing variants may be generated by simple splicing errors, and such proteins are normally degraded by a process termed nonsense-mediated decay (NMD) (1). NMD occurs when a transcript contains a stop codon in a position more than 50–55 nucleotides upstream of the 3′-most exon-exon junction, in which case polysome-associated Upf proteins interact with the exon-junction-protein complex to elicit NMD. In contrast, if translation terminates within 50–55 nucleotides upstream of the 3′-most exon-exon junction or downstream of the junction, mRNA appears to be protected against NMD (45). Based on these parameters, FISP-sp is a product of alternative 3′-splice site splicing, which represents ~8% of total alternative splicing events and is not classified as a splicing error (5). In addition, FISP-sp splicing occurs at an A(G/G)T site, which includes the major class of splicing site sequences (3). Although FISP-sp mRNA contains a premature stop codon, this stop codon is located at the junction of exon 4 and exon 5. Thus, the transcript is not detected as a target for NMD, and FISP-sp protein is maintained in the cell.

RT-PCR analysis shows that the FISP-sp expression levels are 10% of the levels of full-length IL-24/FISP. FISP-sp is localized predominantly in the ER. Overexpression of FISP-sp and FISP together reduced the growth inhibition and apoptosis induced by IL-24/FISP in tumor cells. Analysis of various apoptotic characteristics revealed that FISP-sp not only rescues FISP-induced growth inhibition but also, remarkably, blocks apoptosis induced by FISP (Fig. 4). It was also found that FISP-sp is not secreted, and multiple FISP-sp protein bands detected by Western blot analysis suggest that FISP-sp is highly glycosylated, like FISP. However, because of FISP-sp frameshift splicing, three putative *N*-glycosylation sites, asparagine residues at amino acid positions 170, 195, and 208, are eliminated, and the glycosylation patterns of FISP and FISP-sp might differ. Not only is FISP-sp completely localized in the ER but it also blocks secretion of FISP completely, thereby antagonizing the most important property of FISP as a cytokine with bystander antitumor activity. The inhibition of FISP secretion, the physical interaction of FISP and FISP-sp, and the ER retention of FISP are features that point toward a mechanism by which FISP is exclusively regulated under ER stress conditions (Fig. 5). Further analysis of the fate of the retained FISP protein, via treatment with MG132, a potent proteasome inhibitor, suggested that FISP is efficiently recruited to the proteasome for degradation (Fig. 5*D*). To test whether this degradation is mediated by recruitment of ubiquitin, FISP-transfected and FISP + FISP-sp co-transfected samples were immunoprecipitated with their respective antibodies and analyzed by Western blot using an anti-ubiquitin antibody. Although no dramatic differences were observed, the FISP band appeared to be more prominent in samples from co-transfected cells (supplemental Fig. 5). Protein bands overlapping the IgG light chain (25 kDa) and lower bands around 17 kDa were more prominent in comparison with the samples from cells transfected with FISP only (supplemental Fig. 5). Proteomic analysis identified peptides of proteins involved in ubiquitination, including ubiquitin-activating enzyme E1 and ubiquitin-conjugating enzyme E2 to be FISP-sp/FISP interacting proteins (supplemental Table 1). We also detected the peptides of ubiquitin-specific peptidase 9, which is a deubiquitinating enzyme (46), and LOC629750, a protein similar to ubiquitin A-52 residue ribosomal protein fusion product 1. This protein acts as a protein modifier that can be covalently attached to target lysines, either as a monomer or as a lysine-linked polymer, leading to their degradation by the proteasome. We also detected the peptides of transitional endoplasmic reticulum ATPase (VCP). VCP is a component of a complex that binds ubiquitinated proteins and is necessary for the export of misfolded proteins from the ER to the cytoplasm, where they are degraded by the proteasome (48). Detection of the above proteins in complex with FISP or FISP-sp indicates an association between FISP and FISP-sp in the ubiquitination-mediated proteasomal degradation pathway. Along with unique peptides of FISP-sp and FISP that verify the interaction of FISP and FISP-sp (data not shown), the detection of peptides of two major splice factors, Spfq (proline- and glutamine-rich) and Sprs9 (arginine/serine-rich 9), further supports this interaction and provides a glimpse into the mechanism whereby FISP-sp is generated, and the manner in which FISP and FISP-sp are regulated.

Our results corroborate those recently reported by Gopalan *et al.* (49) demonstrating ubiquitination and subsequent 26 S

proteasome-mediated degradation of MDA-7 in cancer cells. In addition, inhibition of ubiquitination reportedly led to enhanced killing of cancer cells, an effect that might result from accumulation of IL-24 protein. In normal cells, however, FISP degradation might be mediated by its splicing variant FISP-sp, which is up-regulated in stress conditions. Further studies are needed to understand the precise relationship between FISP, FISP-sp, and the ubiquitin-proteasome system.

According to quantitative real time RT-PCR analysis, FISP-sp is expressed at 10% of the total level of primary FISP transcripts detectable in mouse Th2 cells (Fig. 1), which suggests that FISP-sp and FISP coexist. Hence, we propose that FISP-sp function might not be independent of FISP but might instead be coordinated to support or regulate FISP. This idea is strengthened by considering the following question. If apoptosis is caused by IL-24/MDA-7-induced ER stress in T cells, how does a similar accumulation of intracellular IL-24 protein in normal T cells during Th2 lymphocyte differentiation occur without eliciting apoptosis? We hypothesize that FISP-sp is generated in response to FISP-induced ER stress and that it acts to regulate FISP function by blocking ER stress and subsequently apoptosis. In this study, we have shown that FISP-sp levels can be increased by ER stress in NIH3T3 cells and EL-4 cells, as well as in primary Th2 cells, but not in mouse melanoma B16F10.9 cells. These results suggest that the cellular machinery in cancer cells can inhibit the formation of FISP-sp upon ER stress induction (Fig. 6*E*). Transient reporter assays also show a significant increase in FISP-sp levels upon ER stress induction. Moreover, when FISP-sp was co-transfected with FISP, the cell growth inhibition induced by FISP was nullified. It is interesting to note that although overexpressed FISP-sp is localized and accumulated in the ER, unlike FISP it does not induce apoptosis. Unlike FISP, overexpression of FISP-sp alone did not up-regulate ER stress-associated ER chaperones like BiP/GRP78, GRP94, calreticulin, and PDI (supplemental Fig. 2) in B16F10.9 and HeLa cells. FISP-sp rather down-regulated FISP-mediated up-regulation of ER stress-responsive genes, indicating that FISP-sp generation may be a normal physiological process to resolve the ER stress without any negative side effects. These observations seem to contradict the idea that IL-24/MDA-7-mediated apoptosis is caused by its massive accumulation in the ER and raises the question of why IL-24/MDA-7 induces apoptosis in cancer cells but not in normal cells. In other words, if IL-24/MDA-7 induces ER stress in cancer cells, then normal cells would be expected to be similarly affected by ER stress.

Nonconventional mRNA splicing is a well known mechanism by which cellular survival against ER stress is improved. In the case of IRE1-mediated alternative splicing, as reported in yeast HAC1 and human XBP1 transcripts, mRNA introns are spliced by IRE1 endonucleolytic cleavage activity. Under conditions of ER stress, activated IRE1 removes a 26-nucleotide intron from native Xbp1 mRNA. This splicing event generates a frameshift, producing a protein that activates the UPR, which in turn efficiently resolves the ER stress (50).We speculate that alternative splicing and generation of FISP-sp is a survival mechanism against FISP-induced ER stress, and that this mechanism is maintained in normal cells but is dysfunctional in tumor cells. The proportional balance of FISP and FISP-sp expression levels may play a central role in normal cell development. We assume that this is one reason for the observation that FISP induces apoptosis in B16F10.9 cells but not in NIH3T3 cells. Indeed, we did not observe any increase in FISP-sp mRNA levels or FISP-sp protein splicing-dependent luciferase activity in B16F10.9 cells (Fig. 6*E*), which presumably renders the tumor cells more susceptible to FISP-induced growth inhibition. Upon overexpression of the +29-SP-ΔATG-frame3-GFP vector in NIH3T3 cells, GFP signals were detected. Similarly, in HEK293 and EL-4 cells, certain levels of reporter gene activity were found even in untreated cells, but the levels increased when cells were treated with the ER stress inducers tunicamycin and thapsigargin. These results suggest that NIH3T3, HEK293, and EL-4 cells have a mechanism of splicing FISP mRNA to form FISP-sp under naturally occurring conditions of FISP-induced ER stress. In contrast, B16F10.9 cells lack any ability to generate FISP-sp, and thus fail to control ER stress successfully, leading to FISP-induced apoptosis. Moreover, we demonstrated that FISP-sp is generated or up-regulated by FISP-induced ER stress during Th2 cell development. However, whether splicing of FISP to FISP-sp is mediated by IRE1 remains to be tested. The exact mechanism of the failure of tumor cells to inhibit FISP-sp function, which leads to their growth inhibition, remains unclear. Considering the recent report by Gupta *et al.* (23), demonstrating the physical interaction between IL-24/MDA-7 and the ER chaperone BiP/GRP78, further studies are needed to determine whether FISP is involved in such an interaction and to exactly define the biochemical nature of FISP-sp and whether FISP-sp interferes with this interaction to prevent cell death in normal cells.

In summary, we have identified a novel splicing variant of FISP, named FISP-sp, and characterized its induction, subcellular localization, and function as an antagonist of FISP. Our observations, reported here, provide *in vivo* evidence of ER stress-mediated generation and up-regulation of FISP-sp. These findings contribute to our understanding of the physiological regulation of splicing and the functional relationships between splicing product isoforms.

Acknowledgments—We thank our colleagues in the laboratory for contributions to the work and critical review of the manuscript.

REFERENCES

1. Stamm, S., Ben-Ari, S., Rafalska, I., Tang, Y., Zhang, Z., Toiber, D., Thanaraj, T. A., and Soreq, H. (2005) *Gene* (*Amst.*) **344,** 1–20
2. Kriventseva, E. V., Koch, I., Apweiler, R., Vingron, M., Bork, P., Gelfand, M. S., and Sunyaev, S. (2003) *Trends Genet.* **19,** 124–128
3. Philips, A. V., and Cooper, T. A. (2000) *Cell. Mol. Life Sci.* **57,** 235–249
4. Schroder, M., and Kaufman, R. J. (2005) *Mutat. Res.* **569,** 29–63
5. Ast, G. (2004) *Nat. Rev. Genet* **5,** 773–782
6. Schaefer, G., Venkataraman, C., and Schindler, U. (2001) *J. Immunol.* **166,** 5859–5863
7. Soo, C., Shaw, W. W., Freymiller, E., Longaker, M. T., Bertolami, C. N., Chiu, R., Tieu, A., and Ting, K. (1999) *J. Cell. Biochem.* **74,** 1–10
8. Jiang, H., Lin, J. J., Su, Z. Z., Goldstein, N. I., and Fisher, P. B. (1995) *Oncogene* **11,** 2477–2486
9. Madireddi, M. T., Su, Z. Z., Young, C. S., Goldstein, N. I., and Fisher, P. B. (2000) *Adv. Exp. Med. Biol.* **465,** 239–261

10. Mhashilkar, A. M., Schrock, R. D., Hindi, M., Liao, J., Sieger, K., Kourouma, F., Zou-Yang, X. H., Onishi, E., Takh, O., Vedvick, T. S., Fanger, G., Stewart, L., Watson, G. J., Snary, D., Fisher, P. B., Saeki, T., Roth, J. A., Ramesh, R., and Chada, S. (2001) *Mol. Med.* **7,** 271–282
11. Sarkar, D., Su, Z. Z., Lebedeva, I. V., Sauane, M., Gopalkrishnan, R. V., Dent, P., and Fisher, P. B. (2002) *BioTechniques* S30–S39
12. Sauane, M., Gopalkrishnan, R. V., Sarkar, D., Su, Z. Z., Lebedeva, I. V., Dent, P., Pestka, S., and Fisher, P. B. (2003) *Cytokine Growth Factor Rev.* **14,** 35–51
13. Lebedeva, I. V., Sauane, M., Gopalkrishnan, R. V., Sarkar, D., Su, Z. Z., Gupta, P., Nemunaitis, J., Cunningham, C., Yacoub, A., Dent, P., and Fisher, P. B. (2005) *Mol. Ther.* **11,** 4–18
14. Chen, W. Y., Cheng, Y. T., Lei, H. Y., Chang, C. P., Wang, C. W., and Chang, M. S. (2005) *Genes Immun.* **6,** 493–499
15. Allen, M., Pratscher, B., Roka, F., Krepler, C., Wacheck, V., Schofer, C., Pehamberger, H., Muller, M., and Lucas, T. (2004) *J. Investig. Dermatol.* **123,** 583–588
16. Agarwal, S., and Rao, A. (1998) *Immunity* **9,** 765–775
17. Macian, F., Garcia-Cozar, F., Im, S. H., Horton, H. F., Byrne, M. C., and Rao, A. (2002) *Cell* **109,** 719–731
18. Im, S.-H., Hueber, A., Monticelli, S., Kang, K.-H., and Rao, A. (2004) *J. Biol. Chem.* **279,** 46818–46825
19. Iwawaki, T., Hosoda, A., Okuda, T., Kamigori, Y., Nomura-Furuwatari, C., Kimata, Y., Tsuru, A., and Kohno, K. (2001) *Nat. Cell Biol.* **3,** 158–164
20. Bert, A. G., Burrows, J., Osborne, C. S., and Cockerill, P. N. (2000) *Plasmid* **44,** 173–182
21. Lebedeva, I. V., Su, Z., Chang, Y., Kitada, S., Reed, J. C., and Fisher, P. B. (2002) *Oncogene* **21,** 708–718
22. Sauane, M., Gopalkrishnan, R. V., Lebedeva, I., Mei, M. X., Sarkar, D., Su, Z. Z., Kang, D. C., Dent, P., Pestka, S., and Fisher, P. B. (2003) *J. Cell. Physiol.* **196,** 334–345
23. Gupta, P., Walter, M., Su, Z., Lebedeva, I., Emdad, L., Randolph, A., Valerie, K., Sarkar, D., and Fisher, P. (2006) *Cancer Res.* **66,** 8182
24. Chada, S., Sutton, R. B., Ekmekcioglu, S., Ellerhorst, J., Mumm, J. B., Leitner, W. W., Yang, H. Y., Sahin, A. A., Hunt, K. K., Fuson, K. L., Poindexter, N., Roth, J. A., Ramesh, R., Grimm, E. A., and Mhashilkar, A. M. (2004) *Int. Immunopharmacol.* **4,** 649–667
25. Gupta, P., Su, Z.-Z., Lebedeva, I. V., Sarkar, D., Sauane, M., Emdad, L., Bachelor, M. A., Grant, S., Curiel, D. T., Dent, P., and Fisher, P. B. (2006) *Pharmacol. Ther.* **111,** 596–628
26. Sieger, K. A., Mhashilkar, A. M., Stewart, A., Sutton, R. B., Strube, R. W., Chen, S. Y., Pataer, A., Swisher, S. G., Grimm, E. A., Ramesh, R., and Chada, S. (2004) *Mol. Ther.* **9,** 355–367
27. Sauane, M., Lebedeva, I. V., Su, Z. Z., Choo, H. T., Randolph, A., Valerie, K., Dent, P., Gopalkrishnan, R. V., and Fisher, P. B. (2004) *Cancer Res.* **64,** 2988–2993
28. Kerr, J. F. R., Wyllie, A. H., and Currie, A. R. (1972) *Br. J. Cancer* **26,** 239–257
29. Wyllie, A. H. (1992) *Cancer Metastasis Rev.* **11,** 95–103
30. Sarkar, D., Su, Z.-Z., Lebedeva, I. V., Sauane, M., Gopalkrishnan, R. V., Valerie, K., Dent, P., and Fisher, P. B. (2002) *Proc. Natl. Acad. Sci. U. S. A.* **99,** 10054–10059
31. Sauane, M., Gupta, P., Lebedeva, I. V., Su, Z.-Z., Sarkar, D., Randolph, A., Valerie, K., Gopalkrishnan, R. V., and Fisher, P. B. (2006) *Cancer Res.* **66,** 11869–11877
32. Jiang, H., Su, Z. Z., Lin, J. J., Goldstein, N. I., Young, C. S., and Fisher, P. B. (1996) *Proc. Natl. Acad. Sci. U. S. A.* **93,** 9160–9165
33. Sarkar, D., Su, Z., Vozhilla, N., Park, E. S., Randolph, A., Valerie, K., and Fisher, P. B. (2005) *Cancer Res.* **65,** 9056–9063
34. Zhao, L., Gu, J., Dong, A., Zhang, Y., Zhong, L., He, L., Wang, Y., Zhang, J., Zhang, Z., and Huiwang, J. (2005) *Hum. Gene Ther.* **16,** 845–858
35. Su, Z., Sarkar, D., Emdad, L., Duigou, G., Young, C., Ware, J., Randolph, A., Valerie, K., and Fisher, P. (2005) *Proc. Natl. Acad. Sci. U. S. A.* **102,** 1059–1064
36. Lebedeva, I., Su, Z., Sarkar, D., and Fisher, P. (2003) *Semin. Cancer Biol.* **13,** 169–178
37. Fisher, P. B., Gopalkrishnan, R. V., Chada, S., Ramesh, R., Grimm, E. A., Rosengeld, M. R., Curiel, D. T., and Dent, P. (2003) *Cancer Biol. Ther.* **2,** S23–S37
38. Huang, E. Y., Madireddi, M. T., Gopalkrishnan, R. V., Leszczyniecka, M., Su, Z., Lebedeva, I. V., Kang, D., Jiang, H., Lin, J. J., Alexandre, D., Chen, Y., Vozhilla, N., Mei, M. X., Christiansen, K. A., Sivo, F., Goldstein, N. I., Mhashilkar, A. B., Chada, S., Huberman, E., Pestka, S., and Fisher, P. B. (2001) *Oncogene* **20,** 7051–7063
39. Caudell, E. G., Mumm, J. B., Poindexter, N., Ekmekcioglu, S., Mhashilkar, A. M., Yang, X. H., Retter, M. W., Hill, P., Chada, S., and Grimm, E. A. (2002) *J. Immunol.* **168,** 6041–6046
40. Chada, S., Mhashilkar, A. M., Ramesh, R., Mumm, J. B., Sutton, R. B., Bocangel, D., Zheng, M., Grimm, E. A., and Ekmekcioglu, S. (2004) *Mol. Ther.* **10,** 1085–1095
41. Ramesh, R., Mhashilkar, A. M., Tanaka, F., Saito, Y., Branch, C. D., Sieger, K., Mumm, J. B., Stewart, A. L., Boquoi, A., Dumoutier, L., Grimm, E. A., Renauld, J. C., Kotenko, S., and Chada, S. (2003) *Cancer Res.* **63,** 5105–5113
42. Hershko, A., and Ciechanover, A. (1982) *Annu. Rev. Biochem.* **51,** 335–364
43. Ciechanover, A., Orian, A., and Schwartz, A. (2000) *BioEssays* **22,** 442–451
44. Elton, T. S., and Martin, M. M. (2003) *Trends Endocrinol. Metab.* **14,** 66–71
45. Maquat, L. E. (2002) *Curr. Biol.* **12,** R196–R197
46. Chung, C. H., and Baek, S. H. (1999) *Biochem. Biophys. Res. Commun.* **266,** 633–640
47. Deleted in proof
48. Woodman, P. G. (2003) *J. Cell Sci.* **116,** 4283–4290
49. Gopalan, B., Shanker, M., Scott, A., Branch, C. D., Chada, S., and Ramesh, R. (2007)
50. Yoshida, H., Matsui, T., Yamamoto, A., Okada, T., and Mori, K. (2001) *Cell* **107,** 881–891